RSC Advances

PAPER

View Article Online
View Journal | View Issue

Cite this: *RSC Adv.*, 2020, **10**, 43927

Interaction among clays and bovine serum albumin

Martin Mucha,* Roman Maršálek, Marta Bukáčková and Gabriela Zelenková

Interactions between bovine serum albumin and various clays including pure clay minerals and bentonite were studied with the aim to describe the interaction process. The adsorption of albumin on the clays is strongly affected by the behavior of clays in the aquatic environment (hydrolysis and release of cations). A sufficient amount of albumin was adsorbed on the acid-activated montmorillonite K10 (0.067 mg mg^{-1}) and on the illite–smectite (0.086 mg mg^{-1}). These clay minerals do not strongly affect the sorption solution parameters such as pH value and content of cations. Practically no adsorption was observed on the bentonite and vermiculite. Bentonite and vermiculite are subject to stronger interactions with water which cause the increase of pH value of the sorption solution and release of cations to the solution and thus they cause conformational changes of albumin, which was confirmed by circular dichroism measurements. Obtained results were confirmed by infrared spectroscopy and thermal analysis as well. Interaction of studied materials with bovine serum albumin causes the reduction of particle size in the case of all studied clays except vermiculite. Albumin probably attacks the clay structure during the adsorption, which causes the decrease of particle size. The presented work contributes to the knowledge about interaction of bovine serum albumin with clays in the field of influence of physico-chemical behaviour of clays in the solution on the interaction with albumin.

Received 14th February 2020
Accepted 19th November 2020

DOI: 10.1039/d0ra01430c

rsc.li/rsc-advances

Introduction

Targeted pharmaceutical delivery to afflicted tissues is an intensively studied topic nowadays. Silicate based materials, especially clay minerals, are very often utilized for this purpose.[1–12] Clay minerals belong to the group of layered silicates (phyllosilicates) where particular layers are composed of tetrahedral networks which contains mainly silicon in their central positions and octahedral networks containing mainly aluminum, magnesium or Fe(II) or Fe(III). Isomorphic substitution of the central cations takes place, which causes permanent negative charge on the layers. Kaolinites, montmorillonites and vermiculites are the most frequently studied phyllosilicates.[13–15] Clays can be modified by various ways, which brings new and better properties of these materials.[14,15] Frequently the acid activation is performed both for research and industrial purposes. Acid activation leads to the partial dissolution of the layers' structure as well as it leads to the increase of the specific surface area.[16–19] The modification can be done by transformation of the material on the monoionic form or intercalation of the various inorganic and organic molecules to the interlayer space can be performed as well.[14,15] These modified as well as original untreated materials can be utilized for the above mentioned targeted pharmaceuticals delivery or they can be used for the purpose of the continuous pharmaceutical release[1–12] or for the preparation of the antibacterial nanomaterials.[20,21]

Biocompatibility of the newly invented materials can be a serious problem.[20,22] Properties (charge, surface area, swelling properties, ionic exchange or sorption properties) can strongly influence their behavior in the organism. Clays are able to interact with inorganic as well as organic compounds including nonpolar ones. They can interact with cations present in the organism or with protein as well.[9,23–34] Therefore it is necessary to study the biocompatibility of new nanomaterials based on clays and to study the interactions with proteins. Bovine serum albumin (BSA) is frequently utilized as the model compound for this purpose.[23,25–29,32] Studies dealing with adsorption of BSA and other proteins on the kaolinite,[23,35] halloysite,[35] montmorillonite,[9,26,27,32] hollow silica nanospheres[25] or a polymer brush[36] were already published. However, presented results vary significantly in some cases. Yu *et al.*[34] provided in their review value of adsorbed amount 0.16 mg mg^{-1}, Lü *et al.*[27] stated values between 0.37 and 0.39 mg mg^{-1}. However, Lepoitevin *et al.*[26] stated value of adsorbed amount 1.4 mg mg^{-1}. Interactions among proteins and clay minerals are very difficult to describe mainly due to structural changes of the protein according to the pH value of the solution as well as according to presence of various cations in the solution.[37] Clay minerals are subject to hydrolysis frequently. Hydrolysis causes increase of the solution's pH value and various ions are released to the solution due this process.[13,15] These changes can lead to the modifications of the secondary, tertiary and maybe quaternary structures of the BSA, which influences strongly the adsorption of the BSA on the surface of the clay minerals.[37]

Department of Chemistry, Faculty of Science, University of Ostrava, 30. dubna 22, 70103 Ostrava, Czech Republic. E-mail: martin.mucha@osu.cz

Presented work deals with study of interactions among BSA and various clays. Preliminary experiments are focused on the mechanistic study of the interactions at single concentration of the BSA solution. Results were obtained by batch technique. The pH values of all solutions were measured and contents of dissolved SiO_2 and selected cations (Ca, Mg, Fe, Na and K) were determined in the solutions. Results were verified by the infrared spectroscopy. Issues with BSA determination in the solutions are explained, too. The changes of particle size distribution of the clays caused by interaction with BSA solution and changes in the zeta potential at various pH values are discussed. Adsorption kinetics and isotherms were measured for selected clay materials.

Experimental

Clay minerals and their characterization

The following clay materials were used for interaction experiments: montmorillonite, illite, bentonite and vermiculite. Montmorillonite K10 (Mt K10) represents acid activated montmorillonite (Sigma-Aldrich Ltd., Germany). Natural non activated bentonite type B75 (Bent B75) was supplied by fy. Keramost Inc. (Czech Republic). Natural brazilian vermiculite (Ver) was supplied by Grena Inc. (Czech Republic) and illite–smectite type ISMt-1 (abbreviated I–Sm) was supplied by Source Clay Minerals Repository (USA). I–Sm was milled prior the utilization. No other treatments were performed on the used materials. All materials were characterized by the infrared spectroscopy (FTIR) and thermal analysis (TG/DSC). Elemental composition of all used clays was determined by their dissolution in the HCl and HNO_3 according to norm ČSN 72 0106 part 1. Content of SiO_2 was determined gravimetrically by heating of the residue from the materials dissolution at 1000 °C. Contents of Al, Ca, Mg, Na, K and Fe were determined by atomic absorption spectroscopy (AAS). Content of Al was determined utilizing graphite furnace atomization on the Agilent 240Z spectrometer (Agilent Technologies Inc., USA) on the wavelength 256.8 nm. Contents of Ca, Mg, Na, K and Fe were determined on the Varian AA240FS spectrometer (Varian Inc., USA) equipped by flame atomization (air–acetylene flame). The wavelengths were 422.7 nm for Ca determination, 202.6 nm for Mg determination, 372.0 nm for Fe determination, 330.3 nm for Na determination and 769.9 nm for K determination. The highest limit of quantification (LOQ) of the utilized methods was 0.05 mg L^{-1}. Cation exchange capacities were determined by saturation of clays by Na(I) ions with subsequent exchange of these ions by ammonia cations. Clays were five times repeatedly saturated by 0.5 mol L^{-1} solution of NaCl. After saturation they were washed by demineralized water and dried in dryer at 105 °C to the constant weight. Then the saturated clays were exposed repeatedly to the NH_4Cl solution (concentration 0.5 mol L^{-1}) and the solution after contact was collected. The amount of Na(I) ions was determined by the above mentioned AAS method.

Preliminary experiments

Stock solution of BSA (Sigma Aldrich Ltd., Germany) with concentration 2 mg mL^{-1} was prepared. Amount of 0.5 g of studied materials was weighted to the Erlenmeyer flask and 50 mL of BSA solution was added. Dispersions were kept for 24 hours and then centrifuged on the Jouan BR4i centrifuge (Thermo Electron Corp., USA) at 6000 rpm for 15 minutes. Solids after centrifugation were dried at laboratory temperature and they were measured by FTIR spectroscopy. Solutions after centrifugation were measured on the UV-VIS spectrometer Varian Cary 50 (Varian, USA) at 279 nm to obtain concentration of BSA after contact with studied materials and then the solutions were filtered through Pragopor 6 0.4 μm membrane filter (Pragochema, Czech Republic) and they were measured again on the UV-VIS spectrometer. The pH values of the solutions before and after contact were measured on the pH meter InoLab 735 (WTW, Germany) with pH electrode WTW SenTix 41. Blank samples with all studied materials and demineralized water were prepared by the same way as samples with BSA solution for determination of pH values changes and the content of released SiO_2, Ca, Mg, Fe, Na and K caused by interactions of studied materials in the aqueous environment. The content of SiO_2 was determined by UV-VIS spectrometry after reaction of sample with ammonium molybdate on the wavelength 430 nm. The contents of cations in the solutions were determined by above mentioned AAS methods. The amount of BSA adsorbed (a) was determined from the change in the solution concentration before and after equilibrium, according to:

$$a = \frac{(c_0 - c_e) \times V}{m}$$

where c_0 (mg mL^{-1}) is the initial concentration of the BSA solution, c_e (mg mL^{-1}) the concentration of the BSA solution at the adsorption equilibrium, V (mL) the volume of the BSA solution and m (mg) the mass of the clay material.

UV-VIS spectra measurement

The UV-VIS spectra of the BSA solutions (concentration 2 mg mL^{-1}) with different pH values (without adjustment of the pH value – 6.4, pH values 3 and 9) were measured on the UV-VIS spectrometer Varian Cary 50 (Varian Inc., USA). The pH values of the solutions were adjusted by addition of HCl and NaOH solutions (both Mach-Chemicals Ltd., Czech Republic).

Adsorption of BSA

Adsorption experiments were performed only for Mt K10 and I–Sm according to the results of previous experiments. BSA solutions of 50 mL and concentration of 0.7 mg mL^{-1} were prepared to measure kinetics. All adsorption experiments were carried out in sodium phosphate buffered saline solution (PBS), the pH of the solution was 4.4. 50 mg of a clay material was added to the solution. After contact time (30, 60, 90, 120, 150, 180, 210 and 240 minutes) the solutions were centrifuged at 6000 rpm for 15 minutes. The BSA concentrations in the supernatants were determined by UV spectrometry (Cary 50, Varian, USA) at a wavelength of 279 nm. In addition, the effect of initial concentration on BSA adsorption was studied, adsorption isotherms were measured. The initial BSA concentration ranged from 0.1 to 2.0 mg mL^{-1}, the volume of the

sorption solution was 50 mL and the weight of clay material was the 50 mg.

Dynamic light scattering and zeta potential

Size distributions and zeta potential of the clays particles and BSA molecules were determined with a Malvern Zetasizer Nano ZS (Malvern Instruments Ltd., GB). The dynamic light scattering (DLS) technique was used for measurement of particles size distribution. Before the zeta potential measurements, all samples were sonicated for 5 minutes. The Zetasizer Nano ZS uses Laser Doppler Velocimetry to determine electrophoretic mobility. The zeta potential was obtained from the electrophoretic mobility by the Smoluchowski equation. The influence of pH in the range 2–11 was determined.

Infrared spectroscopy

Infrared spectra were collected on the Nicolet 6700 FTIR spectrometer (Thermo Scientific, USA) equipped by KBr beamsplitter and DTGS/KBr detector in the spectral range 4000–400 cm^{-1}. Solid samples (clays before and after contact with BSA) were measured by KBr pellet technique (2 mg of sample was mixed with 250 mg of KBr and pellet was prepared by the usual way). Resolution was set on 4 cm^{-1}, 64 scans were collected, appodization was used Happ–Genzel. Solutions after centrifugation were measured by ATR technique (single bounce diamond crystal). Solutions were evaporated directly on the crystal and solid residue was measured with parameters: 256 scans, resolution 4 cm^{-1}, appodization Happ–Genzel. Each sample was measured twice and spectra were averaged.

Thermal analysis

Thermoanalytical experiments (TG-DSC) of the pristine clays and the materials loaded with BSA were performed using a Setsys Evolution (Setaram, France). The measurements were carried out with 40–46 mg of the sample in the crucible from α-Al_2O_3 without standard. TG-DSC curves were recorded in the dynamic atmosphere (20% of O_2 and 80% of Ar, flow rate 40 mL min^{-1}) from 15–700 °C with the heating rate 10 K min^{-1}.

Circular dichroism

Circular dichroism (CD) measurements of the solutions containing BSA after contact with clays were performed for estimation of changes in the protein secondary structure. Solutions after contact with clay were diluted 10× and measured on the Jasco J-815 CD spectropolarimeter recording wavelength from 190 to 260 nm at room temperature. Measurements were performed in the 1 mm path length cuvette. CD data were measured as CD(obs) in mdeg and expressed in terms of mean residue ellipticity (MRE) in deg cm^2 $dmol^{-1}$:[38,39]

$$\mathrm{MRE} = \frac{\mathrm{CD(obs)}}{C_\mathrm{p} N l}$$

where C_p is the protein molar concentration after the removal of clay material, N the number of amino acid residues in the protein chain (for BSA 583) and l is the path length of used cuvette. The spectra were blank subtracted with distilled water spectra and all samples were measured three times.

The amount of α-helix structure was calculated from the dichroic spectra form this equation:[38,39]

$$\alpha\text{-Helix } (\%) = \frac{-\mathrm{MRE}_{208} - 4000}{33\,000 - 4000} \times 100$$

where MRE_{208} is the mean residue ellipticity at characteristic minimum for α-helix.

SEM photographs

SEM photographs were taken on the JEOL JSM-6610LV microscope equipped with backscattered electron detector. Following parameters were set up for the measurement: accelerating voltage 18 kV, working distance 14 mm, spot size 30 and magnification 5000×.

Results and discussion

Source materials characterization

The spectra of the studied source materials used for experiments are shown on the Fig. 1. Mt K10 represents a silicate material (Si–O stretch vibration band at 1056 cm^{-1}). It is possible to observe shift of this band by about 20 cm^{-1} to the higher wavelengths if compared to the I–Sm and Bent B75 spectra. This shift is probably caused by the acid activation of the Mt K10 material which leads to the partial disintegration of the Mt layers.[16,18] The disintegration is incomplete, a portion of the Mt remains unchanged, which can be inferred from the band 3629 cm^{-1} (stretch vibration of O–H bond in the structural hydroxyl groups of Mt). The material contains free water as well (bands about 3400 cm^{-1} and 1632 cm^{-1}). Material I–Sm is constituted by a smectite component, presumably Mt, which can be inferred from the presence of the structural vibration band at 3625 cm^{-1} which is typical for Mt. The structural –OH groups of the illite (I) exhibit a weak shoulder around 3700 cm^{-1}. The position of the Si–O stretch vibration band (1032 cm^{-1}) indicates the content of Mt in the material, the shoulder at 1079 cm^{-1} belongs to the Si–O vibration of the I. Compared to the Mt K10 material, the I–Sm contains less water (this can be deduced from the absorbance of the bands around 3400 and 1632 cm^{-1}), and also contains the highest amount of quartz compared to other studied materials (bands in the range 800–750 cm^{-1}). Bent B75 consists mainly of Mt (bands 1036, 3621 cm^{-1}) but it contains other components as well: kaolinite/illite (3698 cm^{-1}), carbonates (1480 cm^{-1}), quartz (bands in the range 800–750 cm^{-1}). It also contains higher amount of free water. Ver is a structurally different material compared to the previous ones. The different structure can be assumed from the Si–O bond vibration (999 cm^{-1}) and O–H stretch vibration bands positions (around 3700 cm^{-1}). The band of free water (around 3400 cm^{-1}) is very broad compared to other materials, which can be related to the structure of the material. Vermiculites exhibit high charge of the layers which is compensated by interlayer hydrated cations. The hydration shells form an octahedral network.[40,41] The interactions among clays and BSA could be realized by structural hydroxyl groups (3620–

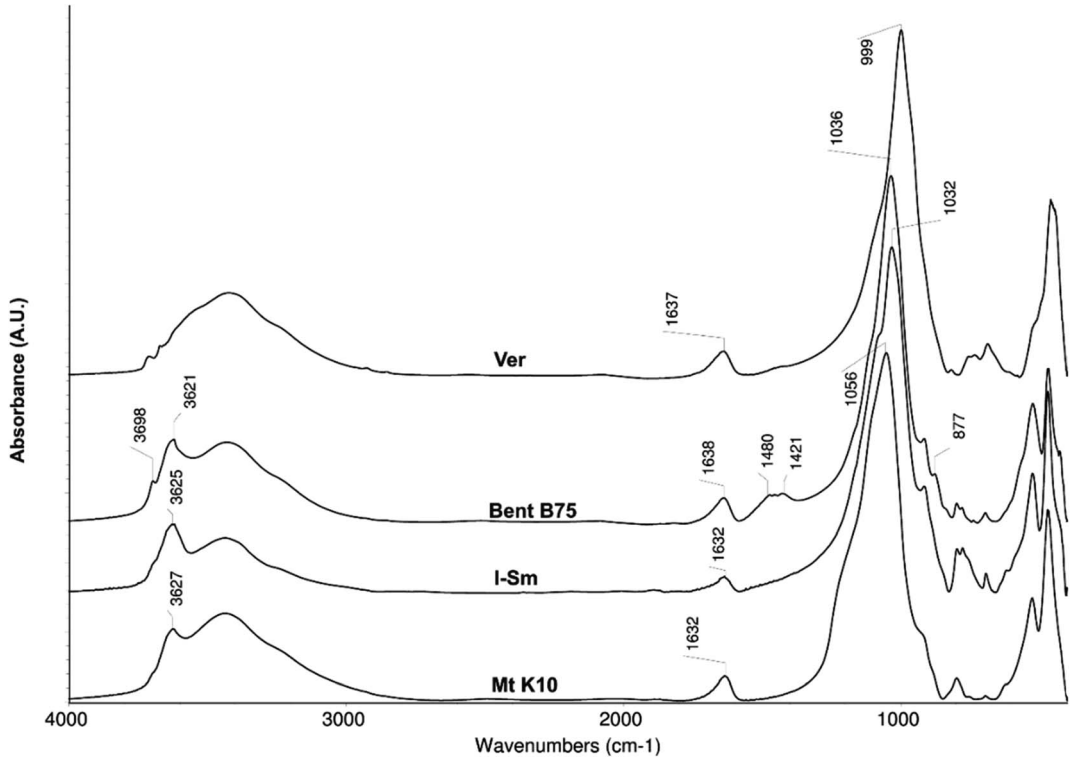

Fig. 1 Infrared spectra of used materials.

3630 cm^{-1}) through the formation of cation bridges with the carboxylic groups from the BSA molecules or the interactions can be electrostatic among negatively charged clay surface and partially positively charged parts of BSA molecules.

Elemental composition of the utilized clays as well as cation exchange capacities are shown in the Table 1. It is evident that materials Mt K10 and I–Sm have higher content of SiO_2 compared to Bent B75 and Ver materials. On the other hand, contents of Ca, Mg and Fe are significantly higher for the Bent B75 and Ver materials compared to Mt K10 and I–Sm. Mt K10 represent acid activated montmorillonite, which confirm the higher amount of SiO_2 and lower amount of cations. The higher content of cations which can be released to the solution in the Bent B75 and Ver clays can explain the pH values changes observed during the contact of clays with BSA. Different behaviour of the Bent B75 and Ver compared to Mt K10 and I–Sm in the contact of the clays with BSA solution can be caused by the layer charge of the materials as well. The Bent B75 and Ver clays exhibit significantly higher values of cation exchange capacities in the comparison to Mt K10 and I–Sm, thus the charge can affect the structure of BSA as well as the repulsion of clays and negatively charged parts of BSA molecules.

Preliminary adsorption experiments

The content of BSA was determined in solution after centrifugation (6000 rpm, 15 min). Then the solutions were filtered through a 400 nm nitrocellulose membrane filter and the BSA content in the solutions was determined again. The adsorbed amount a (Table 2) was calculated from the obtained data. It can be seen that BSA has been bonded to the surface of the Mt K10 and I–Sm but it is not adsorbed on the Bent B75 and Ver (the calculated values are even negative). The obtained information

Table 1 Elemental composition of the used clays and cation exchange capacities (CEC)

	Mt K10	I–Sm	Bent B75	Ver
SiO_2 [% w/w]	78.279 ± 2.553	87.837 ± 0.307	54.469 ± 1.100	51.268 ± 0.420
Al_2O_3 [% w/w]	5.438 ± 0.442	1.738 ± 0.043	7.716 ± 1.155	8.710 ± 1.756
CaO [% w/w]	0.178 ± 0.010	0.210 ± 0.024	1.984 ± 0.452	0.603 ± 0.105
MgO [% w/w]	0.962 ± 0.026	0.338 ± 0.005	3.629 ± 0.030	15.298 ± 0.204
Na_2O [% w/w]	0.065 ± 0.002	0.044 ± 0.008	0.740 ± 0.083	0.748 ± 0.050
K_2O [% w/w]	0.227 ± 0.009	0.427 ± 0.144	0.300 ± 0.068	3.347 ± 0.775
Fe_2O_3 [% w/w]	2.346 ± 0.057	0.649 ± 0.030	12.402 ± 1.412	6.626 ± 0.352
CEC [meq g^{-1}]	0.343 ± 0.028	0.314 ± 0.011	0.628 ± 0.013	0.825 ± 0.020

Table 2 Adsorbed amount in the preliminary experiment after centrifugation and filtration

Clay	$a_{centrifugation}$ [mg mg^{-1}]	$a_{filtration}$ [mg mg^{-1}]
Mt K10	0.058	0.059
I–Sm	0.057	0.049
Bent B75	−0.037	−0.002
Ver	−0.002	0.000

corresponds to the infrared spectroscopy data shown further. The determined adsorbed amount after filtration was almost the same as after centrifugation in case of Mt K10. However, the observed adsorbed amount on the I–Sm after filtration was reduced in the comparison with value obtained for solution after centrifugation. Negative values obtained for Bent B75 and Ver are reduced for the filtrates, too. Interactions among studied materials and BSA probably result in the formation of supramolecular structures (as indicated below by FTIR study). These supramolecular structures can cause scattering of measuring beam during determination (determination was conducted by UV spectroscopy) and thus a positive determination error. Therefore, the adsorbed amount of BSA on the Bent B75 and Ver seems to be equal to zero. Zero adsorption of BSA on the Bent B75 and Ver clays can be caused by higher layer charge of these clays in the comparison to the Mt K10 and I–Sm. Negative charge can lead to the repulsion of the clays' surface and negatively charged parts of the BSA molecules.

Fig. 2 shows changes in pH value before and after the contact of BSA with clay materials. It can be seen that Mt K10 and I–Sm cause a decrease of pH value during sorption (the pH value of the BSA solution before mixing with the Mt K10 and I–Sm was higher than the pH of the solution after centrifugation). Bent B75 and Ver show the opposite behaviour when the pH value is significantly increased after contact. The pH value of the solution affects the conformation of the BSA and thus also probably its ability to bind to the clay material. The acidic groups contained in the BSA will be dissociated at higher pH values as well and the formation of the supramolecular structures by the binding *via* the multivalent cations could be much easier. The

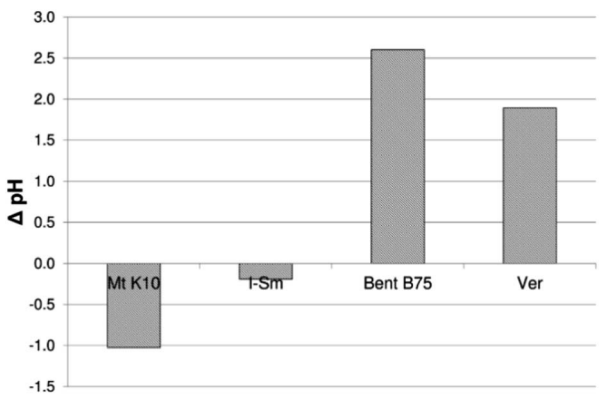

Fig. 2 Changes in the pH value due to interaction of studied materials with BSA.

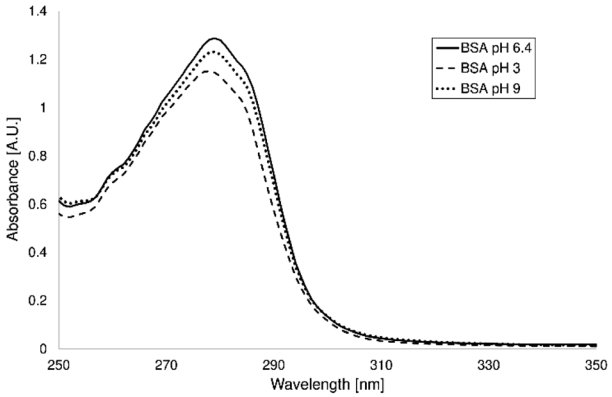

Fig. 3 UV-VIS spectra of BSA in the aquatic solution at various pH values.

pH value changes fully correspond to the lower adsorption rate. The lower pH value of the solution after sorption means the higher adsorbed amount of BSA on the clay surface. In alkaline conditions the formation of large (>400 nm) conglomerates of BSA molecules probably occurs in the solution.

Spectra of the BSA only in the aquatic solution at various pH values were measured to describe the effect of the pH value on the UV-VIS spectra (Fig. 3). It is evident that the change of the pH value of the solution has very weak effect on the spectra. The shape of the spectral bands is almost the same in the case of all studied pH values. The slightly different absorbances are probably caused by pH value adjustment because solution of HCl or NaOH was added to the solution of BSA for adjustment, so the concentration of BSA slightly decrease.

The content of selected cations, soluble silicates and pH values of the solutions after contact of the studied clays with demineralised water are shown in Table 3. The pH value of the demineralized water was 5.4. The pH of the solution after contact with Mt K10 was lower than that of demineralized water. It is an acid-activated mineral that contains acidic groups in its structure. They dissociate upon contact with water and cause a decrease in pH value. In I–Sm, the pH remained practically unchanged after contact with demineralized water. Bent B75 and Ver significantly increase the pH value of the solution after contact. The changes of pH values after the contact of clays with demineralized water are comparable with pH values after

Table 3 Released amounts of selected species from the utilized materials during contact with demineralized water and change of the pH value of the solution during contact of used materials with demineralized water. LOQ – limit of quantification

	Released amount [mg g^{-1}]						
Sample	SiO_2	Ca	Mg	Fe	Na	K	ΔpH
Mt K10	1.62	0.01	0.02	<LOQ	0.07	0.04	−1.03
I–Sm	0.17	<LOQ	<LOQ	<LOQ	<LOQ	0.05	0.04
Bent B75	1.47	<LOQ	0.03	0.52	3.37	0.47	3.98
Ver	0.92	<LOQ	0.02	0.01	1.41	0.11	3.79

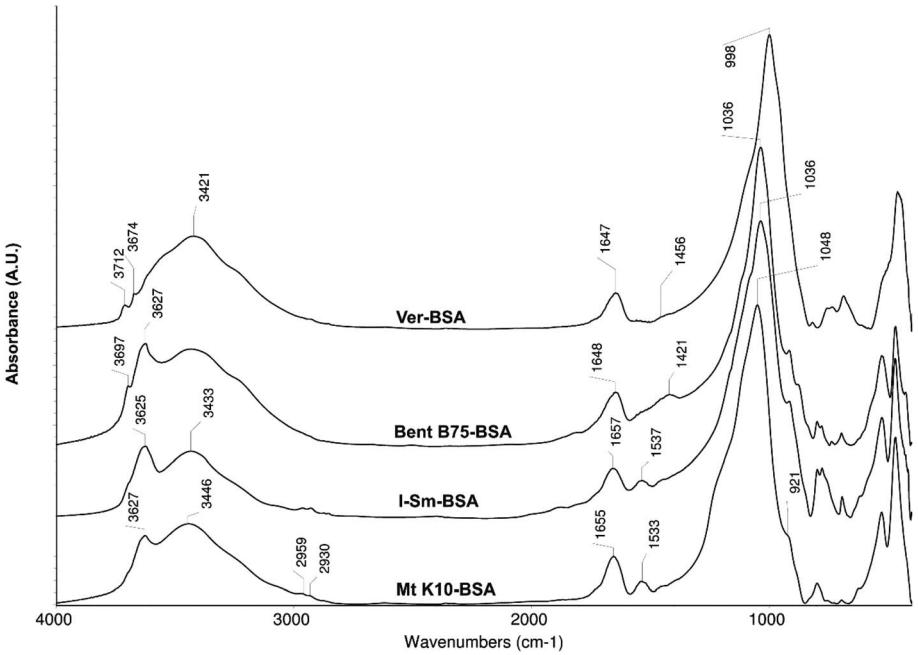

Fig. 4 Spectra of studied materials after contact with BSA.

sorption of BSA in the case of Mt K10 and I–Sm. Differences between changes of pH values in the case of Bent B75 and Ver could be caused by dissociation of the acidic groups of BSA in the alkaline environment. Changes in Bent B75 and Ver solutions are probably related to the hydrolysis of the minerals forming the materials as can be concluded from the contents of released species shown in the Table 3. The amount of released SiO_2 is around 1.5 mg g^{-1} in the case of Mt K10 and Bent B75. The released amount of SiO_2 from I–Sm is about 1 order lower compared to other studied materials and content of released cations is much lower, too. I–Sm is probably much more stable (due to mixing of Mt and illitic layers and higher content of quartz proved by FTIR spectroscopy) and it is not subject to hydrolysis. The content of released cations is very low (around 0.14 mg g^{-1}) in the case of Mt K10 as well. It can be stated that during contact of Mt K10 are released mainly silicates disrupted during acidic activation but almost no cations are released to the demineralized water. On the other hand, the released amounts of cations are around 4.39 mg g^{-1} and 1.55 mg g^{-1} in the case of Bent B75 and Ver. Higher amount of released species can affect the structure of the BSA as well as pH value of the solution and thus ability for bonding to the clay surface. Obtained amounts of released cations correlate with adsorbed amount of BSA therefore it can be stated that released cations influence strongly the sorption process.

Fig. 4 shows the spectra of individual utilized clay materials after contact with the BSA solution. For Mt K10 and I–Sm, new bands around 2959 and 2930 cm^{-1} can be observed which belong to the stretch vibrations of C–H bonds in the BSA molecules. The band around 1535 cm^{-1} can be assigned a BSA molecule as well (valence vibrations C=C in the aliphatic and aromatic parts of the molecule and the deformation vibrations of the –NH group). These bands are not present in the Bent B75 and Ver spectra. It can be suggested that BSA is not adsorbed on the surface of the two last mentioned materials. The only observable change in the Bent B75 spectrum before and after contact with BSA is the change in shape and absorbance (reduction) of the band around 1421 cm^{-1}, which belongs to the carbonates. The acidic groups in the BSA molecule probably interact with the carbonates present in the Bent B75. Increase of free water content is observable as an aqueous solution of BSA was used for the experiment. In the case of Ver, no changes are observable in the spectrum except the increase of the absorbance of the free water bands (3400 and 1647 cm^{-1}), which indicate an increase of its content in the material. In case of Mt K10 and I–Sm, BSA binding to the surface of clay mineral is confirmed by infrared spectroscopy.

Fig. 5 shows spectra of the solids (solid residue after evaporation of water) from the sorption solutions after contact of clay–BSA. All solutions after contact with clay materials and after centrifugation contain only BSA (no subsequent filtration was performed for this measurement). The spectra differ mainly in the area of the stretch vibrations of the carbonyl group (C=O, 1731 cm^{-1}), and in the region of the stretch vibrations of C=C bond and the deformation vibrations of –NH bonds (1541 cm^{-1}). The bands in the range of –CH deformation vibrations (1453, 1395 cm^{-1}) and C–O stretch vibrations (1300–1100 cm^{-1}) vary as well. Differences in spectra are most likely due to small conformational changes of the BSA molecule caused by contact with clay. The previous results correspond to changes in C=O bond vibration band (1731 cm^{-1}). Solutions where BSA was bound to the surface of clay contain in their spectra of residual BSA content a band of this vibration. Solutions where the bonding did not occur do not contain the band

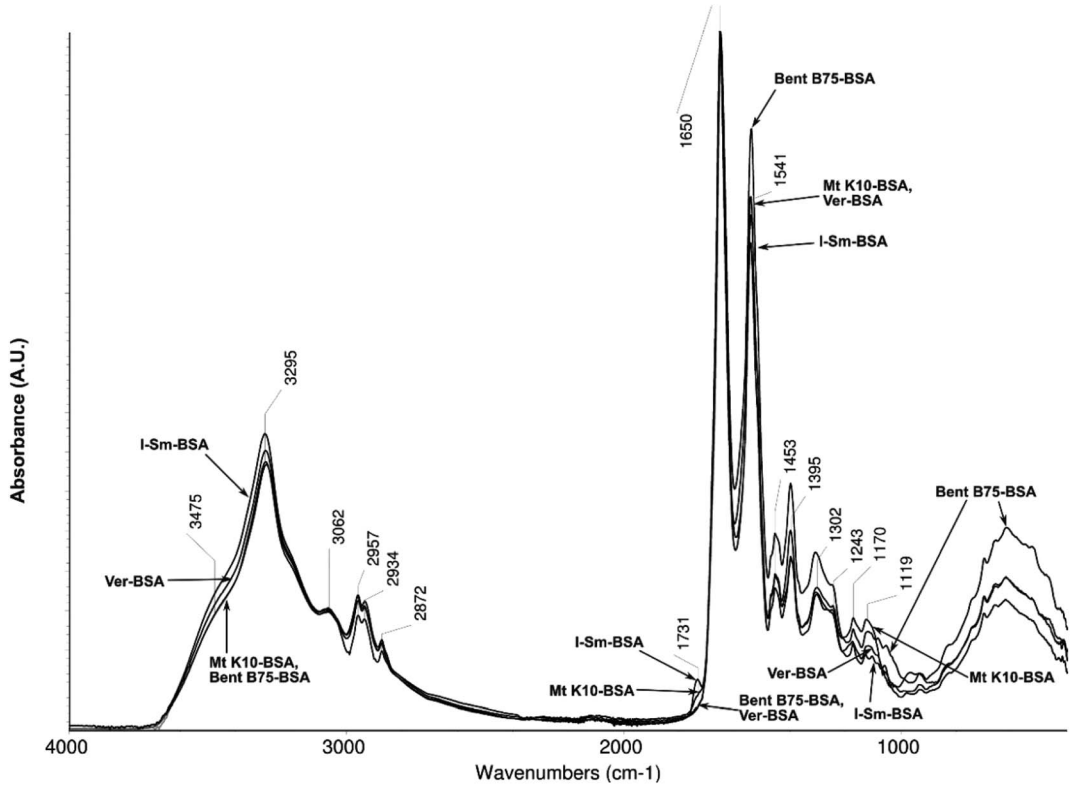

Fig. 5 Spectra of the content of solutions after contact of clays with BSA after evaporation of water.

in the spectrum. These vibrations of carbonyl groups can be assigned to the free carboxylic acids groups of acidic amino acids contained in BSA. Bent B75 and Ver release the cations to the solution during the interaction. These cations probably bind to the free carboxyl groups, which leads to the carboxylates formation. Carboxylates formation is accompanied by the shift of the carbonyl band to the lower wavenumbers and therefore the carboxylate related band is hidden in the aromates C=C band (1650 cm^{-1}). Released cations can thus mediate intramolecular and intermolecular linkages among the different parts of the molecule or among several molecules, thus causing conformational changes or the formation of supramolecular structures that affect BSA binding to clay material.[41]

Circular dichroism measurements were performed for estimation of changes in the secondary structure of protein. CD spectra of solutions containing BSA after contact with clays are shown on the Fig. 6. It can be concluded from the spectra that BSA has highly ordered structure containing α-helices (negative bands at 208 and 222 nm and positive band at 193 nm, Table 4) as well as β-sheets (negative band at 218 nm and positive at 195 nm).[42] BSA in all solutions after contact with clay material shows the changes of protein secondary structure. The measured CD spectra are the same for untreated BSA, Mt K10 and I–Sm, but for these samples the concentration of BSA in solution after contact with the clay is lower. This mean that the percentage representation of BSA α-helices is higher than in case of untreated BSA. The same it is with the samples of BSA after contact with Bent B75 and Ver. These two samples do not

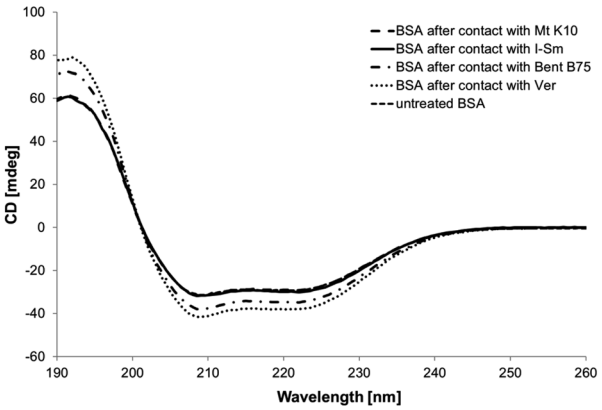

Fig. 6 Circular dichroism spectra of BSA solutions after contact with clays and untreated BSA.

interact with protein, so the final concentration is the same as initial and there can be seen that the CD spectrum is lower. After calculation the amount of BSA α-helix is also higher. The calculated results exhibited a rise of α-helical structures from 60.2% (untreated BSA) to 70.9% (BSA–Mt K10), 72.7% (BSA–Bent B75), 76.5% (BSA–I–Sm) and 80.5% (BSA–Ver).

The obtained data confirm structural changes of BSA caused probably by higher pH value and released cations in the case of contact with Bent B75 and Ver. These changes can cause the inability of BSA to adsorb on the surface of these clays. The

Table 4 CD values [mdeg] at specific wavelengths

	193 nm	195 nm	208 nm	218 nm	222 nm
BSA–Mt K10	59.46279	51.98086	−30.74511	−28.97733	−29.19868
BSA–I–Sm	58.14169	52.46866	−31.24251	−29.58983	−30.06898
BSA–Bent B75	70.34759	61.47676	−36.93531	−34.55133	−34.89178
BSA–Ver	76.70569	67.54206	−40.89791	−37.93603	−37.93688
BSA	58.14169	52.46866	−30.6172	−29.1805	−29.2617

obtained data confirm the influence of clays to the structural changes of proteins, too.

The thermal properties (TG-DSC) of the albumin/clays composites are shown in Fig. 7. The first observable and dominant endothermic mass losses (up to ∼200 °C) are related to the release of the water (interparticle, adsorbed and interlayer). The experimentally determined mass losses of this step from TG curve were 9.6% (Mt K10), 8.10% (BSA Mt K10), 2.5% (I–Sm), 2.2% (BSA I–Sm), 10.2% (Bent B75) and 9.3% (BSA–Bent B75). In the case of the Ver sample, the dehydration step (up to ∼240 °C) is composed from the two parts (two endothermic peaks on the DSC curve, see Fig. 7). This behaviour can be observed for the ungrounded type of the vermiculite.[43] The two step dehydration of the Ver sample resulted in a 4.8% and 0.7% (Ver) and 5.2% and 0.8% (BSA–Ver) mass loss.

With the increasing heating temperature, the degradation of the adsorbed albumin and the dehydroxylation (endothermic release of the –OH groups from the structure in the form of water) of the clays samples occur.

The degradation of the bovine albumin in the albumin/clay sample is observable in the case of the Mt K10, I–Sm and Bent B75 sample. The albumin degradation occurs in the temperature range of 260–400 °C (300–400 °C for Bent B75 sample) and is accompanied with the exothermic effect on DSC signal. The results obtained from the TG-DSC measurement are in good correspondence with the adsorption experiments of the bovine albumin on the studied clay samples (0.067 mg mg^{-1} for Mt K10 and 0.086 mg mg^{-1} for I–Sm). According to the TG-DSC experiments, the Bent 75 sample adsorb a little amount of the bovine albumin too (∼1% mass change connected with the exothermic effect on DSC). Unfortunately, this was not confirmed by the adsorption experiments, probably because of the difficulties connected with the determination of the concentrations changes in such a low scale.

SEM photographs

The SEM photographs of materials Mt K10 and Bent B75 are depicted on the Fig. 8. The photographs of I–Sm and Ver lead to the same conclusions therefore they are not shown here. It is evident that particles of BSA can not be seen on the materials after contact of clays with BSA solution. The contact of clays with solution of BSA leads only to the aggregation of the clay particles, which is common for suspensions of clays.[44] The

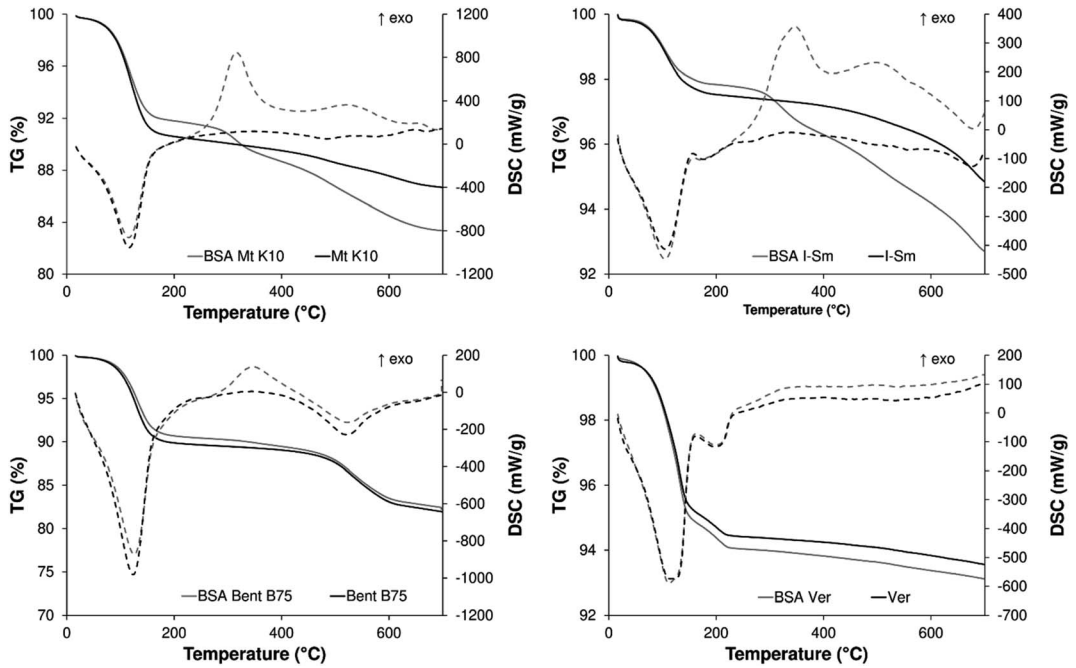

Fig. 7 TG/DSC curves of studied clays before and after contact with BSA.

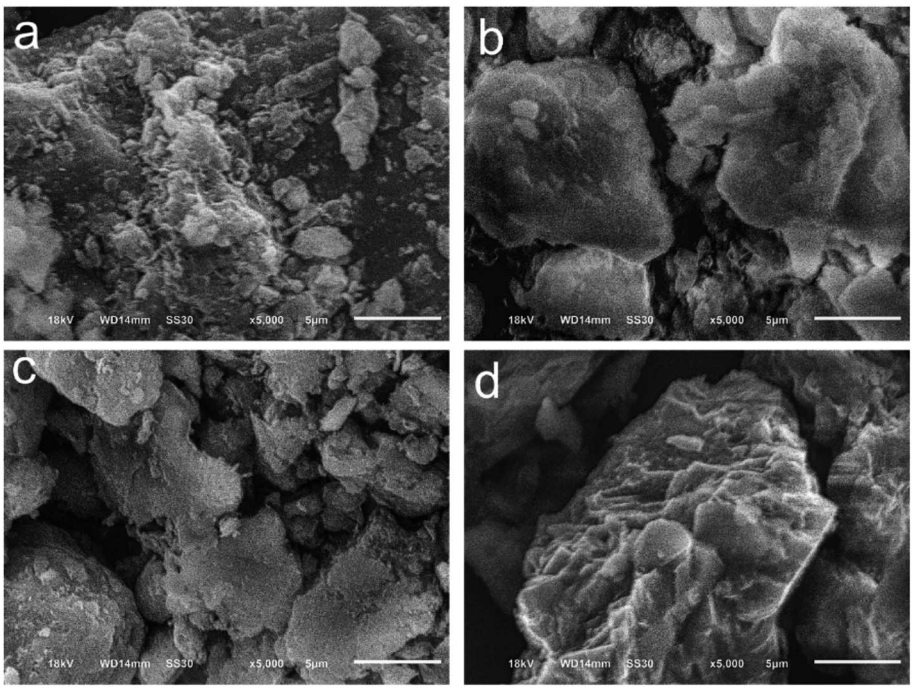

Fig. 8 SEM photographs of Mt K10 (a), Mt K10–BSA (b), Bent B75 (c) and Bent B75–BSA (d).

aggregation can be caused by drying and crushing of the materials prior the SEM measurement. It can be concluded that SEM photographs can not contribute to clarification of BSA–clay interaction.

Adsorption properties of BSA

When observing the time required to achieve the adsorption equilibrium or to saturate the surface of the clay material, samples were taken for analysis after 30, 60, 90, 120, 150, 180, 210 and 240 minutes. The results are shown in Fig. 9.

Fig. 9 shows the adsorption kinetics of BSA on two clays: Mt K10 and I–Sm. The course of adsorption is very similar and is based on the well-known fact that the composition and structure of these minerals is similar, I–Sm being composed up of about 70% of Mt. The rapid increase in adsorption can be observed at the beginning and the equilibrium is reached after approximately 90 minutes. Similar results were obtained by Lepoitevin *et al.*[26]

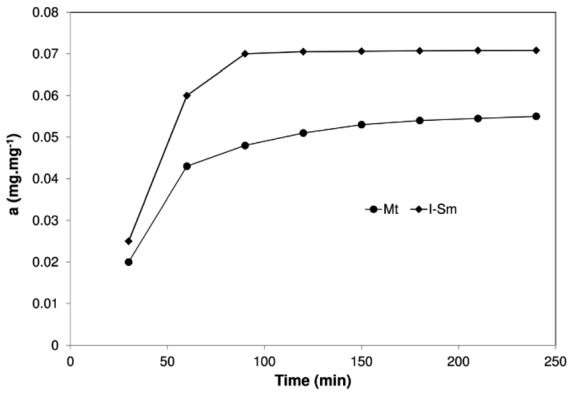

Fig. 9 Adsorption kinetics of BSA at pH 4.4 adsorbed on Mt K10 (circles) and I–Sm (diamonds).

Two kinetic models were used to explain the mechanism of the adsorption processes. The pseudo-first-order kinetic model is given by the Lagergren equation:[45,46]

$$\log(a_e - a_t) = -\frac{k_1}{2303}t + \log a_e$$

where a_e and a_t are the amounts of BSA adsorbed (mg g^{-1}) at equilibrium time and any time t (hour), respectively, and k_1 is the rate constant of adsorption (min^{-1}).

The plot of $\log(a_e - a_t)$ *versus* t gives a straight line for the first-order adsorption kinetic which allows calculation of the rate constant k_1.

The pseudo-second-order model based on equilibrium adsorption is expressed as:[45,46]

$$\frac{t}{a_t} = \frac{1}{k_2 a_e^2} + \frac{1}{a_e}t$$

where k_2 is the pseudo-second-order rate constant (g mg^{-1} min^{-1}). The equilibrium adsorption capacity (a_e) and the rate constant (k_2) can be determined experimentally from the slope and intercept of plot t/a_t *versus* t.

Several kinetic models (pseudo-first-order model, pseudo-second-order model, Bangham's equation, intra-particle diffusion equation, Elovich equation) are available to understand the behaviour of adsorbents and also to examine the adsorption mechanism and test the experimental data. Previous studies[25,45–47] show that adsorption of BSA onto various adsorbents is mostly described as a process of the pseudo-second

Table 5 Pseudo-first-order and pseudo-second-order kinetic parameters for adsorption of BSA on the clays

	Pseudo-first-order constant			Pseudo-second-order constant		
Clay	k_1 (10^{-3} min^{-1})	a_e (mg mg^{-1})	R^2	R^2	k_2 (10^{-3} g mg^{-1} min^{-1})	a_e (mg mg^{-1})
Mt K10	0.039	1.289	0.68	0.97	22.402	0.068
I–Sm	0.058	3.947	0.84	0.95	17.119	0.086

order model. In this study only two popular kinetic models, pseudo-first-order and pseudo-second-order kinetic model were compared. It is evident from the Table 5 that the calculated linear regression determination coefficients (R^2) are closer to one in the case of pseudo-second-order model for both clays. The calculated values of the adsorbed amount agree better with experimental data as well (see below). These results indicate that the adsorption of BSA on clays followed pseudo-second-order kinetics.

Several well-known models, the so-called Langmuir's isotherm, Freundlich's isotherm, the BET's isotherm, and many others are usually used to evaluate the adsorption. Compliance with the model is judged by statistical tools, linear regression is most often performed and the determination coefficient value is monitored. Fig. 10 shows adsorption isotherms of BSA on the clays at the pH value of sorption solution 4.4.

The maximum saturation state was reached during the isotherm measurement. Such a pattern is typical of Langmuir's isotherm. The determination coefficient in the case of the linearized Freundlich isotherm was only around 0.7 for both clays in the comparison to linearized Langmuir isotherm with determination coefficient 0.96 for Mt K10 and 0.99 for I–Sm respectively.

The Langmuir equation is expressed as:

$$a = \frac{a_m b c_e}{1 + b c_e}$$

where a_m (mg mg^{-1}) is the maximal adsorption capacity of the solute; b (L mg^{-1}) is the adsorption equilibrium constant.

A linear form of the Langmuir isotherm:

$$\frac{c_e}{a} = c_e \frac{1}{a_m} + \frac{1}{a_m b}$$

The maximal adsorption capacity for a given system can be determined from the linearized Langmuir's isotherm. The calculated values are 0.067 mg mg^{-1} for Mt K10, 0.086 mg mg^{-1} for I–Sm. These values are comparable to the results of Barral *et al.*,[48] they studied the adsorption of BSA onto kaolinite. On the other hand, these values are orderly lower compared to the research by Causserand *et al.*[49] and M. Lepoitevin *et al.*[26]

Zeta potential and particle size distribution

Fig. 11 shows the effect of pH on zeta potential of BSA, Mt K10 and I–Sm. The course of zeta potential dependence is typical. In the case of clays, the zeta potential values lie in the negative region for all the pH values observed. An isoelectric point of BSA can be evaluated. Its value was calculated to pH 4.5. The isoelectric point (pH 4.4) was selected for realization of adsorption experiments described above. It can be concluded that negatively charged surface of studied clays interacts with BSA molecule without charge during the adsorption at the pH value 4.4. Sample I–Sm exhibits lower absolute value of the zeta potential at this pH in the comparison with Mt K10 with the highest absolute value (the most negative charge). It could be suggested that pH value under the isoelectric point of BSA can lead to the better adsorption as the BSA is charged positively at these pH values and clays' surface is charged negatively but low pH values can lead to the partial dissolution of the clays structure, which can lower the adsorption by reducing the negative charge in the opposite. The dissolution of structure can lead to release of bigger amount of ions to the solution which can interact with BSA as well. The effect of pH value on the

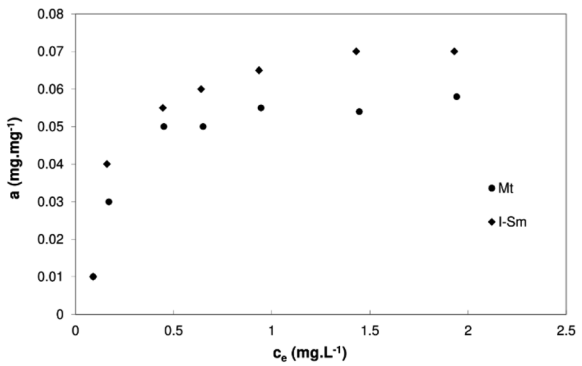

Fig. 10 Adsorption isotherms of BSA at pH 4.4 adsorbed on Mt K10 (circles) and I–Sm (diamonds).

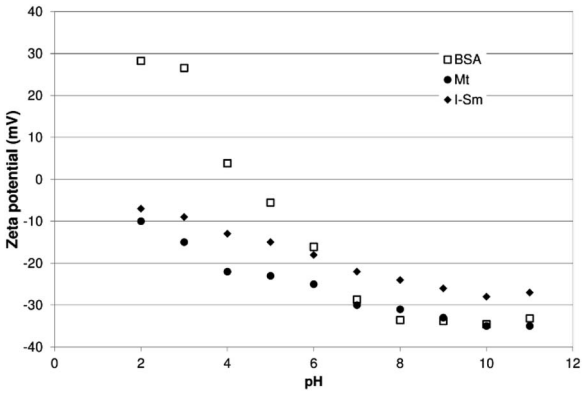

Fig. 11 The influence of pH on zeta potential of BSA (empty squares), Mt K 10 (circles) and I–Sm (diamonds).

Table 6 Particle size distribution and zeta-potential of the studied systems at pH 4.4

Sample name	*Z*-Average (nm)	Number mean (nm)	Volume mean (nm)	*D* (*n*, 50) (nm)	*D* (*v*, 50) (nm)	Zeta potential (mV, pH 4.4)
BSA	465.7	6.6	7.8	6.4	7.2	2.0
I–Sm	3577.9	2177.3	2374.5	2131.7	2350.8	−14.0
I–Sm + BSA	1957.7	672.4	1637.9	561.9	1487.7	−5.0
Mt K10	6222.7	1656.9	1724.6	1639.2	1712.5	−22.0
Mt K10 + BSA	3592.5	877.0	1161.9	826.9	1071.6	−15.0
Bent B75	4382.3	2328.9	3402.7	2105.2	3496.7	−10.0
Bent B75 + BSA	1995.8	438.2	2424.5	290.7	2380.4	−9.4
Ver	1187	718.4	1484	647	1370	−8
Ver + BSA	1147	551.2	2263	414	2080	−9

adsorption was not studied further in this study and it can be good idea for further research.

Table 6 summarizes the results from measurements of the particle size distribution of utilized clays and the zeta potential of clays and sorption systems with BSA at pH 4.4.

The default parameter obtained by the dynamic light scattering method is the hydrodynamic diameter of the particle (*Z*-average in the Table 6). It represents the average particle size. The *Z*-average value is based on the intensity of scattered light. The processing software allows the conversion of *Z*-average value and expression of the size distribution in the form of the particles volume distribution or amounts of particles with the individual size fractions. The number mean represents the diameter of the particles which are the most frequent in the measured system. The volume mean specifies the diameter of particles which are the most common from the sight of particles' volume. Value *D* (*n*, 50) is the median of the particle size evaluated according to number of particles with particular diameter and value *D* (*v*, 50) is the median of particle size according to particles' volume.

In the case of clay minerals, changes in their structure occurred during the adsorption of BSA, which was reflected, among other things, in the distribution of particle size. This trend is observable for most of the parameters describing particle size distribution in the Table 6. The differences are reflected in the intensity of this phenomenon in individual clays. The greatest change can be observed by Bent B75, followed by I–Sm and the lowest decrease in the particle size is reported for Ver. The decrease of *Z*-average parameter after interaction is 54% for Bent B75, 45% for I–Sm and 42% for Mt K10. The exception is Ver which did not exhibit any change in the average particle size. For parameter *D* (*n*, 50) the changes are most significant, namely 86% for Bent B75, 74% for I–Sm and 50% for Mt K10. In the case of Ver, the values are even higher compared to initial material. It is necessary to take into account the high level of polydispersity of the sample and the limitations that result from using the DLS technique. The results show that BSA molecules penetrate intensively into the structure of the clay layers and it could cause the exfoliation of the layers.

Adsorption resp. interaction of BSA molecules with clay materials manifests in zeta potential change values, too. These changes are not significant, however, they are consistent with the adsorption data obtained (Fig. 10). Maximal adsorbed amounts of BSA are low compared to other adsorption systems. It appears that after binding of protein molecules to the structure of clay, it is partially disrupted and part of BSA molecules is released back into the solution and no further adsorption occurs.

Conclusions

Interaction among clays and BSA seems to be very complex process affected by structural changes of the BSA molecule. Four clays (acid activated montmorillonite K10, illite–smectite, bentonite B75 and vermiculite) were tested for the interaction with BSA solution. Clays were characterized by the infrared spectroscopy and TG/DSC analysis. The sorption of BSA was tested at concentration level 2 mg mg^{-1}. The preliminary experiment shows that sorption of BSA on the studied materials is strongly influenced by the behaviour of the materials in the aqueous environment. Clays influence the pH value of the solution as well as they release cations to the solution due to hydrolysis of structure. Conformation of BSA molecule is strongly affected by pH value of the solution and cations can probably influence the structure of BSA and these changes can lead to the formation of supramolecular structures. Conformational changes and supramolecular structures influence the binding of BSA on the clay surface. Montmorillonite K10 and illite–smectite are subject to very weak hydrolysis, only slight amount of cations is released to the solution and there is sufficient amount of BSA adsorbed on the clays' surfaces. On the other hand, bentonite B75 and vermiculite are subject to stronger hydrolysis, pH values in the contact with solutions increase to 9 and higher amount of cations is released to the solution in the comparison to montmorillonite K10 and illite–smectite, which cause adsorbed amount practically equal to 0. The structural changes of the protein were confirmed by circular dichroism measurements. Adsorption kinetic and isotherms for montmorillonite K10 and illite–smectite at pH 4.4 were measured. Adsorption of BSA on both clays corresponds to

the pseudo-second-order kinetic model and the equilibration time was 90 minutes. The Langmuir isotherm model is suitable for description of equilibrium sorption data and the maximal adsorbed amounts from the Langmuir isotherm were 0.067 mg mg^{-1} for montmorillonite K10 and 0.086 mg mg^{-1} for illite–smectite. The zeta-potential measurements were performed for BSA and montmorillonite K10 and illite–smectite. The isoelectric point of BSA was determined on the pH value 4.5 and it was determined that both clays are negatively charged in whole studied range of pH values. Zeta-potentials and particle distributions were measured for all studied systems (clays, BSA and clays after contact with BSA) at pH 4.4. It was found out that average particle size of the clays decreases after contact with BSA solution in all cases except of Vermiculite. BSA in the solution probably attacks the clays' surface, which leads to the particle size reduction as well as this phenomenon probably influences sorption od BSA on the clays surface due to structural changes of BSA. Interaction among clays and BSA in the aquatic environment is strongly influenced by the stability of the clay structure.

Conflicts of interest

There are no conflicts to declare.

Acknowledgements

This study was supported by the Ministry of Education, Youth and Sports of the Czech Republic in the ''National Feasibility Program I", project LO1208 "TEWEP", by the EU structural funding Operational Programme Research and Development for Innovation, project no. CZ.1.05/2.1.00/19.0388 and by the project of Faculty of Science, University of Ostrava, no. SGS06/PrF2016-2017, "Zeta potential determination of Bovine Serum Albumin and study of its (BSA) interaction with nanoparticles".

Notes and references

1 M. Baek, J.-H. Choy and S.-J. Choi, *Int. J. Pharm.*, 2012, **425**, 29.
2 H. Bera, S. R. Ippagunta, S. Kumar and P. Vangala, *Mater. Sci. Eng., C*, 2017, **76**, 715.
3 I. Calabrese, G. Cavallaro, C. Scialabba, M. Licciardi, M. Merli, L. Sciascia and M. L. Turco Liveri, *Int. J. Pharm.*, 2013, **457**, 224.
4 I. Calabrese, G. Gelardi, M. Merli, M. L. T. Liveri and L. Sciascia, *Appl. Clay Sci.*, 2017, **135**, 567.
5 R. I. Iliescu, E. Andronescu, C. D. Ghitulica, G. Voicu, A. Ficai and M. Hoteteu, *Int. J. Pharm.*, 2014, **463**, 184.
6 S. Jain and M. Datta, *Appl. Clay Sci.*, 2015, **104**, 182.
7 S. Jain and M. Datta, *J. Drug Delivery Sci. Technol.*, 2016, **33**, 149.
8 S. Jayrajsinh, G. Shankar, Y. K. Agrawal and L. Bakre, *J. Drug Delivery Sci. Technol.*, 2017, **39**, 200.
9 H. Kaygusuz and F. B. Erim, *React. Funct. Polym.*, 2013, **73**, 1420.
10 S. Lal, A. Perwez, M. A. Rizvi and M. Datta, *Appl. Clay Sci.*, 2017, **147**, 69.
11 P. Gnanamoorthy, S. Anandhan and V. A. Prabu, *J. Porous Mater.*, 2014, **21**, 789.
12 P. Singh and K. Sen, *J. Porous Mater.*, 2017, **25**, 965.
13 M. E. Essington, *Soil and Water Chemistry: An Integrative Approach*, CRC Press, Boca Raton, 2004.
14 M. Valášková, *Vybrané vrstevnaté silikáty a jejich modifikované nanomateriály*, CERM, Brno, 2014.
15 Z. Weiss and M. Kužvart, *Jílové minerály: jejich nanostruktura a využití*, Karolinum, Prague, 2005.
16 F. Bergaya and G. Lagaly, *Handbook of Clay Science*, Elsevier, Amsterdam, 2013.
17 F. Hussin, M. K. Aroua and W. M. A. W. Daud, *Chem. Eng. J.*, 2011, **170**, 90.
18 V. Krupskaya, S. Zakusin, E. Tyupina, O. Dorzhieva, A. Zhukhlistov, P. Belousov and M. Timofeeva, *Minerals*, 2017, **7**, 49.
19 F. R. Valenzuela Díaz and P. S. Santos, *Quim. Nova*, 2001, **24**, 345.
20 B. Krishnan and S. Mahalingam, *Adv. Powder Technol.*, 2017, **28**, 2265.
21 A. Roy, B. S. Butola and M. Joshi, *Appl. Clay Sci.*, 2017, **146**, 278.
22 J. Huang, P. Dong, W. Hao, T. Wang, Y. Xia, G. Da and Y. Fan, *Appl. Clay Sci.*, 2014, **313**, 172–182.
23 R. Duarte-Silva, M. A. Villa-García, M. Rendueles and M. Díaz, *Appl. Clay Sci.*, 2014, **90**, 73.
24 T. Felbeck, S. Moss, A. Botas, M. Lezhnina, R. Ferreira, L. Carlos and H. U. Kynast, *Colloids Surf., B*, 2017, **157**, 373.
25 M.-J. Hwang, O.-H. Kim, W.-G. Shim and H. Moon, *Microporous Mesoporous Mater.*, 2013, **182**, 81.
26 M. Lepoitevin, M. Jaber, R. Guégan, J.-M. Janot, P. Dejardin, F. Henn and S. Balme, *Appl. Clay Sci.*, 2014, **95**, 396.
27 Y. Lü, H. Yan, D. Gao, C. Hu and X. Kou, *J. Wuhan Univ. Technol., Mater. Sci. Ed.*, 2013, **28**, 1236.
28 P. M. Schmidt and E. C. Martinez, *Langmuir*, 2016, **32**, 7719.
29 H. Quiquampoix, S. Staunton, M.-H. Baron and R. G. Ratcliffe, *Colloids Surf., A*, 1993, **75**, 85.
30 G. Sanjay and S. Sugunan, *J. Porous Mater.*, 2008, **15**, 359.
31 S. Staunton and H. Quiquampoix, *J. Colloid Interface Sci.*, 1994, **166**, 89.
32 T. Tran and B. J. James, *Colloids Surf., A*, 2012, **414**, 104.
33 T.-Y. Tsai, C. Hsu, V. Chao, S. Huang, C. Chan, T. Wu and P. Wang, *J. Chin. Chem. Soc.*, 2015, **62**, 562.
34 W. H. Yu, N. Li, D. S. Tong, C. H. Zhou, C. X. Lin and C. Y. Xu, *Appl. Clay Sci.*, 2013, **80–81**, 443.
35 V. Della Porta, E. Bramanti, B. Campanella, M. R. Tiné and C. Duce, *RSC Adv.*, 2016, **6**, 72386.
36 H. Kawakita, H. Masunaga, K. Nomura, K. Uezu, I. Akiba and S. Tsuneda, *J. Porous Mater.*, 2006, **14**, 387.
37 S. Servagent-Noinville, M. Revault, H. Quiquampoix and M.-H. Baron, *J. Colloid Interface Sci.*, 2000, **221**, 273.
38 A. Iovescu, A. Băran, G. Stîngă, A. R. Cantemir-Leontieş, M. E. Maxim and D. F. Anghel, *J. Photochem. Photobiol., B*, 2015, **153**, 198.

39 H. Xu, N. Yao, H. Xu, T. Wang, G. Li and Z. Li, *Int. J. Mol. Sci.*, 2013, **14**, 14185.
40 M. Hayati-Ashtiani, *Part. Part. Syst. Charact.*, 2011, **28**, 71.
41 G. Socrates, *Infrared and Raman Characteristic Group Frequencies: Tables and Charts*, Wiley, Chichester, 2004.
42 N. J. Greenfield, *Nat. Protoc.*, 2006, **1**, 2876.
43 V. Balek, J. L. Pérez-Rodríguez, L. A. Pérez-Maqueda, J. Šubrt and J. Poyato, *J. Therm. Anal. Calorim.*, 2007, **88**, 819.
44 E. Tombácz, G. Filipcsei, M. Szekeres and Z. Gingl, *Colloids Surf., A*, 1999, **151**, 233.
45 A. Rathinam and L. Zou, *J. Hazard. Mater.*, 2010, **184**, 597.
46 Z. Wang, T. Yue, Y. Yuan, R. Cai, C. Niu and C. Guo, *Int. J. Biol. Macromol.*, 2013, **58**, 57.
47 N. P. Sasidharan, P. Chandran and S. Sudheer Khan, *Colloids Surf., B*, 2013, **102**, 195.
48 S. Barral, M. A. Villa-García, M. Rendueles and M. Díaz, *Acta Mater.*, 2008, **56**, 2784.
49 C. Causserand, Y. Kara and P. Aimar, *J. Membr. Sci.*, 2001, **186**, 165.